Journal of Physics: Conference Series **592** (2015) 012030 doi:10.1088/1742-6596/592/1/012030

# Studies of $^{27}$Al NMR in $EuAl_4$

**H Niki[1], S Nakamura[1], N Higa[1], H Kuroshima[1], T Toji[1], M Yogi[1], A Nakamura[1], M Hedo[1], T Nakama[1], Y Ōnuki[1] and H Harima[2]**

[1] Department of Physics, Faculty of Science, University of the Ryukyus, Nishihara, Okinawa 903-0213, Japan

[2]Graduate School of Science, Kobe University, Nada-ku, Kobe 657-8501, Japan

E-mail: niki@sci.u-ryukyu.ac.jp

**Abstract.** $EuAl_4$ orders antiferromagnetically at $T_N \approx 16$ K with an effective magnetic moment of 8.02 $\mu_B$. In the paramagnetic phase, the magnetic susceptibility of $EuAl_4$ follows the Curie-Weiss law with a positive Curie-Weiss temperature $\theta_P = +14$ K. The antiferromagnetic state is changed into the field induced ferromagnetic state at a critical field $H_c$ of approximately 2 T. In order to microscopically investigate the magnetic and electronic properties in $EuAl_4$, the NMR measurements of $EuAl_4$ have been carried out at temperatures between 2 and 300 K, applying an external magnetic field of approximately 6.5 T. The $^{27}$Al NMR spectra corresponding to Al(I) and Al(II) sites are obtained. From the $^{27}$Al NMR spectra, the isotropic part $K_{iso}$ and anisotropic part $K_{aniso}$ of Knight shift, and nuclear quadrupole frequncy $\nu_Q$ are obtained. The $K_{iso}$ and $K_{aniso}$ shift to negative side with decreasing temperature due to the RKKY interaction. These temperature dependences follow the Curie-Weiss law with $\theta_P = +14$ K, which is consistent with that of the magnetic susceptibility. From the $K - \chi$ plot, the values of the hyperfine fields $H_{hf\_iso}$ and $H_{hf\_aniso}$ are –3.231 and –0.162 kOe/$\mu_B$ for Al(I) site, and –1.823 and –0.264 kOe/$\mu_B$ for Al(II) site, respectively. The values of $\nu_Q$ of $^{27}$Al nucleus for Al(I) and Al(II) sites are approximately 0.865 and 0.409 MHz, respectively. The nuclear relaxation time $T_1$ of $^{27}$Al NMR for both sites is almost constant in the paramagnetic phase, while the value of $1/T_1$ is abruptly decreased in the ordered ferromagnetic state.

## 1. Introduction

Eu is a rare-earth element known to have two kinds of valence states: $Eu^{2+}$ ($4f^7$) and $Eu^{3+}$ ($4f^6$). The divalent Eu state is magnetic ($J = S = 7/2$, $L = 0$), where $J$ is the total angular momentum, $S$ is the spin angular momentum, and $L$ is the orbital angular momentum. Therefore, the compounds with divalent Eu ions tend to order magnetically, following the Ruderman-Kittel-Kasuya-Yosida (RKKY) interaction. On the other hand, the trivalent Eu state is non-magnetic ($J = 0$, $S = L = 3$).

The divalent Eu intermetallic compound $EuX_4$ (X = Al and Ga) crystallizes in the $BaAl_4$-type structure ($I4/mmm$) as shown in Fig. 1 [1, 2]. Eu atoms occupy the corners and the center of the body-centered tetragonal lattice with local symmetry ($4/mmm$). X atoms (X = Al and Ga) have two crystallographically inequivalent sites, denoted X(I) and X(II), respectively, as indicated in Fig. 1. $EuAl_4$ and $EuGa_4$ orders antiferromagnetically at $T_N \approx 16$ K with effective magnetic moments of 8.02 and 7.86 $\mu_B$, respectively, which are close to a divalent value of 7.94 $\mu_B$/Eu [3, 4, 5]. In the paramagnetic (PRM) phase, the magnetic susceptibilities of $EuAl_4$ and $EuGa_4$ follow the Curie-Weiss law with positive Curie-Weiss temperatures $\theta_P = +14$ and +3 K, respectively [3, 4, 6]. The antiferromagnetic (AFM) states in $EuAl_4$ and $EuGa_4$ are changed

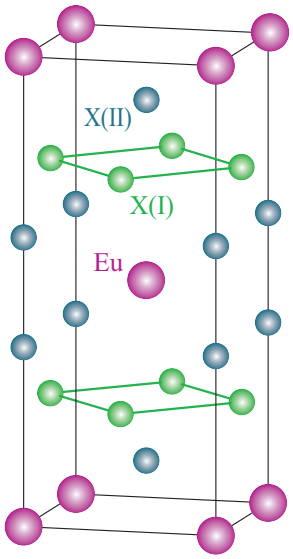


**Figure 1.** (a) Crystal structure of $EuX_4$ (X = Al and Ga).

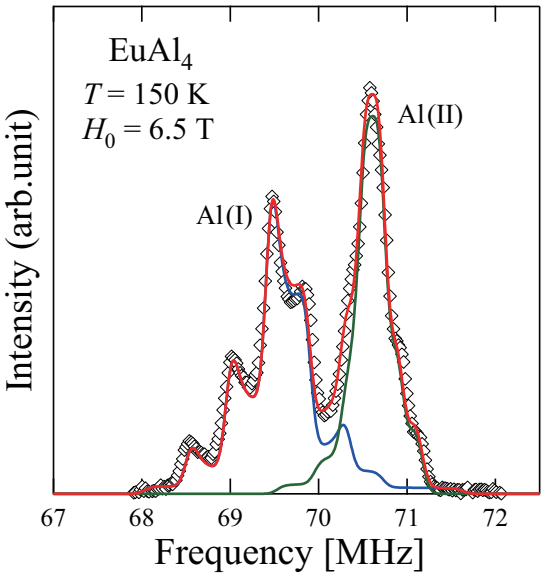


**Figure 2.** $^{27}$Al spectra for Al(I) and Al(II) sites in $EuAl_4$ at 150 K. The solid curves indicate the theoretical curves for the Al spectra analyzed using the Hamiltonian in eq. (1).

into the field induced ferromagnetic (FRM) states at critical fields $H_c$ of approximately 2 and 7 T, respectively [3, 4]. The charge density wave (CDW) transition is occurred around 140 K in $EuAl_4$ [4]. In order to investigate the magnetic property of $EuAl_4$ in the PRM state, NMR measurement has been carried out. In this paper, we report on the magnetic and electronic properties of $EuAl_4$ in the PRM state gained through $^{27}$Al NMR measurements.

## 2. Experimental

Single crystal of $EuAl_4$ was grown by the Al self-flux method. Details of the sample preparation are described elsewhere [1, 2]. The small pieces of the crystal were powdered to facilitate applied rf-field penetration. The $^{27}$Al NMR measurements were performed by a spin-echo method using a conventional phase-coherent pulsed spectrometer. A magnetic field of approximately 6.5 T for $^{27}$Al NMR measurements was applied by a superconducting magnet with magnetic field homogeneity of $10^{-5}$. The NMR spectra were obtained by sweeping the frequency and integrating the spin-echo signal intensity step by step.

## 3. Results and Discussion

The typical NMR spectra of the $^{27}$Al are shown in Fig. 2. The nuclear spin Hamiltonian in the PRM state is given by

$$\mathcal{H} = -\gamma_n \hbar \boldsymbol{I} \cdot \boldsymbol{H}_0 - \gamma_n \hbar \boldsymbol{I} \cdot \boldsymbol{H}_{in} + \frac{h\nu_Q}{6}\left[3I_z^2 - I^2\right] = -\gamma_n \hbar \boldsymbol{I} \cdot \boldsymbol{H}_0 \left[1 + K(\theta)\right] + \frac{h\nu_Q}{6}\left[3I_z^2 - I^2\right]. \quad (1)$$

The first term of the Hamiltonian represents the Zeeman interaction between the nuclear magnetic moment $\boldsymbol{\mu}_n = \gamma_n \hbar \boldsymbol{I}$ and the external magnetic field $\boldsymbol{H}_0$, where $\gamma_n$ is the nuclear gyromagnetic ratio and $\boldsymbol{I}$ is the nuclear spin. The nuclear spin of $^{27}$Al is 5/2. The second term indicates the Zeeman interaction between the nuclear magnetic moment $\boldsymbol{\mu}_n = \gamma_n \hbar \boldsymbol{I}$ and the

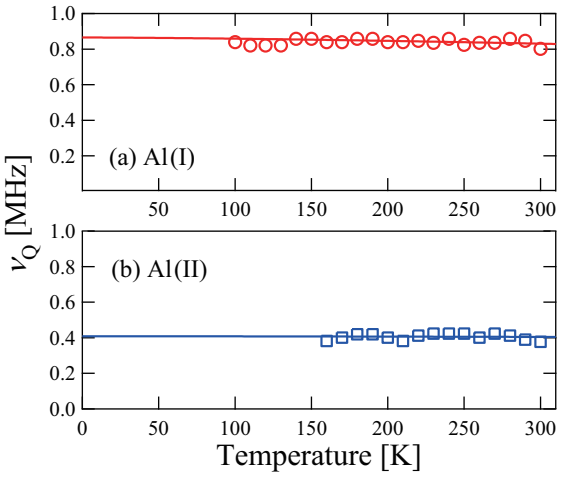


**Figure 3.** Temperature dependence of $^{27}$Al nuclear quadrupole frequency $\nu_Q$ in $EuAl_4$. Figs. (a) and (b) show the $\nu_Q$ for Al(I) and Al(II) sites, respectively. The solid lines in Figs. (a) and (b) indicate the theoretical curves for the $\nu_Q$ values analyzed using the empirical equation expressed by eq. (2).

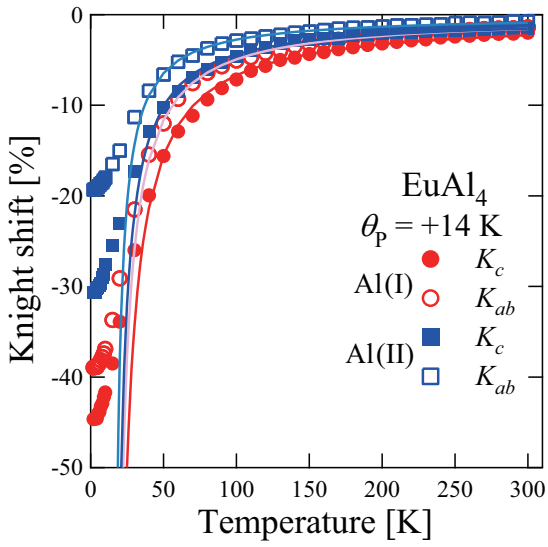


**Figure 4.** Temperature dependences of $^{27}$Al Knight shifts $K_{ab}$ and $K_c$ for Al(I) and Al(II) sites in $EuAl_4$.

internal magnetic field $\boldsymbol{H}_{\rm in}$; this term corresponds to the Knight shift term. If the symmetry of the environment of a nuclear spin is lower than the cubic symmetry, the Knight shift depends on the direction of the applied field with respect to the crystalline axes. In the case of the tetragonal symmetry, the Knight shift is a function of $\theta$, where $\theta$ represents the angle between the external magnetic field and the $c$-axis. The third term indicates the nuclear quadrupole interaction between the electric field gradient (EFG) and the nuclear quadrupole moment $Q$. As for $EuAl_4$, the EFG of the nuclear quadrupole interaction becomes axially symmetric because the crystal structure of $EuAl_4$ has the tetragonal symmetry. Therefore, the asymmetry parameter of the EFG, $\eta$, becomes zero and the EFG along the main principal axis, $V_{zz}$, is parallel to the $c$-axis. Thus, $\nu_Q$ is the nuclear quadrupole frequency defined as $\nu_Q \equiv 3eQV_{zz}/2I(2I-1)h$. The obtained $^{27}$Al NMR spectra have been analyzed using the Hamiltonian in eq. (1). The solid curves in Fig. 2 indicate the theoretical curves for the $^{27}$Al spectra.

Figures 3 (a) and (b) indicate the temperature dependences of $\nu_Q$ for Al(I) and Al(II) sites, respectively. The atomic sites of Al(I) and Al(II) are identified by comparison with $\nu_Q$ obtained from the theoretical calculation, as mentioned below. The experimental values gained from the $^{27}$Al spectra shown in Fig. 3 is fitted by using the following empirical equation [7, 8],

$$\nu_Q(T) = \nu_Q(0)\left(1 - \alpha T^{\frac{3}{2}}\right). \tag{2}$$

The values of $\nu_Q(0)$ and $\alpha$ are $\nu_Q(0) = 0.865$ MHz and $\alpha = 7.75\times10^{-6}$ MHz/K$^{3/2}$ for Al(I) site, and $\nu_Q(0) = 0.409$ MHz and $\alpha = 1.91\times10^{-6}$ MHz/K$^{3/2}$ for Al(II) site, respectively. The fitting results are shown by the solid lines in Fig. 3. The theoretical values of $\nu_Q$ of $^{27}$Al in $EuAl_4$ are calculated based on the band calculation by a full potential linear augmented plane wave (FLAPW) method on the basis of a local density approximation (LDA) assuming without spin-orbit interaction [5, 6]. The calculated values of $\nu_Q$ of $^{27}$Al in $EuAl_4$ are 0.873 MHz for Al(I) site and 0.353 MHz for Al(II) site. Therefore, the obtained $\nu_Q(0)$ values of 0.865 and 0.409 MHz are assigned to the Al(I) and Al(II) sites, respectively.

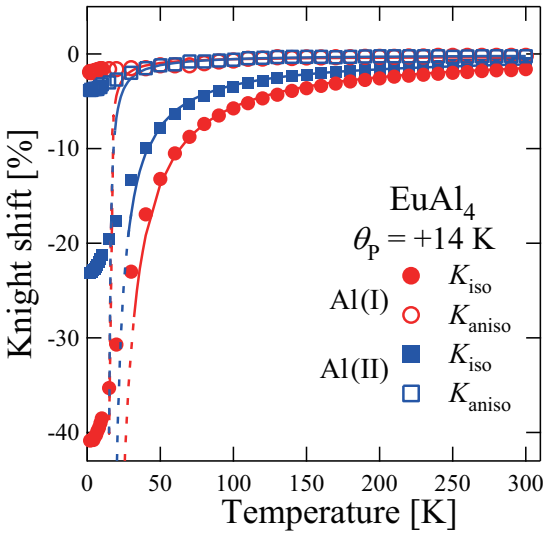


**Figure 5.** Temperature dependences of $^{27}$Al Knight shifts $K_{\rm iso}$ and $K_{\rm aniso}$ at Al(I) and Al(II) sites in $EuAl_4$.

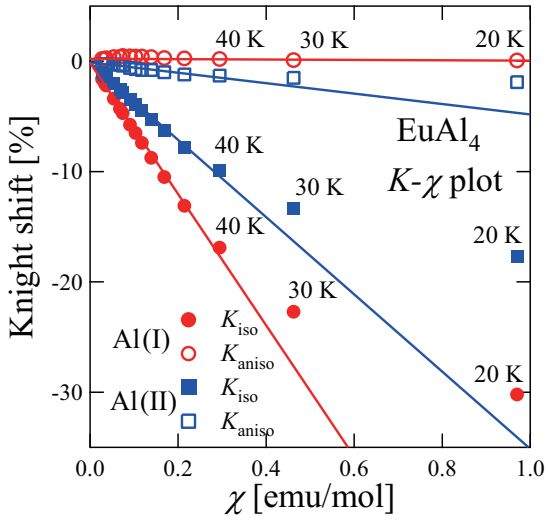


**Figure 6.** $K-\chi$ plots of $^{27}$Al Knight shifts $K_{\rm iso}$ and $K_{\rm aniso}$ at Al(I) and Al(II) sites in $EuAl_4$. The values of hyperfine fields $H_{\rm hf\_iso}$ and $H_{\rm hf\_aniso}$ are –3.231 and –0.162 kOe/$\mu_{\rm B}$ at Al(I) site, and –1.823 and –0.264 kOe/$\mu_{\rm B}$ at Al(II) site, respectively.

The Knight shifts $K_c$ and $K_{ab}$ of $^{27}$Al NMR for both Al(I) and Al(II) sites have been obtained from the $^{27}$Al spectra, as shown in Fig. 4. Here, $K_c$ and $K_{ab}$ are the Kinght shifts in the case of $H \parallel c$-axis and $H \perp c$-axis, respectively [9, 10, 11]. The temperature dependences of the Knight shifts $K_c$ and $K_{ab}$ for both sites shift rapidly to negative side with decreasing temperature, following the the Curie-Weiss law with $\theta_{\rm P} = +14$ K.

Next, we discuss the anisotropy of the $^{27}$Al Knight shift of $EuAl_4$. The isotropic part $K_{\rm iso}$ and anisotropic part $K_{\rm aniso}$ of the Knight shift are obtained from $K_c$ and $K_{ab}$, where $K_{\rm iso} = 1/3\ (K_c + 2\ K_{ab})$ and $K_{\rm aniso} = 1/3\ (K_c - K_{ab})$ [9, 10, 11]. The Knight shift $K_{\rm iso}$ of $^{27}$Al NMR spectra for both Al(I) and Al(II) sites shifts to negative side with decreasing temperature, whereas $K_{\rm aniso}$ shifts just a little to negative side with deceasing temperature, as shown in Fig. 5. The temperature dependences of both $K_{\rm iso}$ and $K_{\rm aniso}$ for both Al sites follow the Curie-Weiss law with $\theta_{\rm P} = +14$ K. The ratio $K_{\rm aniso}(T)/K_{\rm iso}(T)$ is 4.95 % for Al(I) site and 14.90 % for Al(II) site, which corresponds to the ratio of the Curie-Weiss parts of both Knight shifts. The anisotropic part in the Knight shift is small compared with the isotropic part and especially very small for Al(I).

As the magnetic susceptibility in the paramagnetic state is isotropic [2], the temperature dependent terms of Knight shifts $K_{\rm iso}$ and $K_{\rm aniso}$ are expressed in the following equations, respectively,

$$K_{\rm iso}\,(T) = \frac{H_{\rm hf\_iso}}{N\mu_B}\chi\,(T)\,, \tag{3}$$

$$K_{\rm aniso}\,(T) = \frac{H_{\rm hf\_aniso}}{N\mu_B}\chi\,(T) \tag{4}$$

where $N$ is an Avogador's number and $\chi(T)$ is the temperature dependent term of the magnetic susceptibility. Therefore, it is expected that the ratio $K_{\rm aniso}(T)/K_{\rm iso}(T)$ is the same as the ratio $H_{\rm hf\_aniso}/H_{\rm hf\_iso}$. The $K-\chi$ plots for $K_{\rm iso}$ and $K_{\rm aniso}$ for both Al(I) and Al(II) sites are shown in Fig. 6. The hyperfine fields of $^{27}$Al nuclei are obtained from $K-\chi$ plots for $K_{\rm iso}$ and $K_{\rm aniso}$.

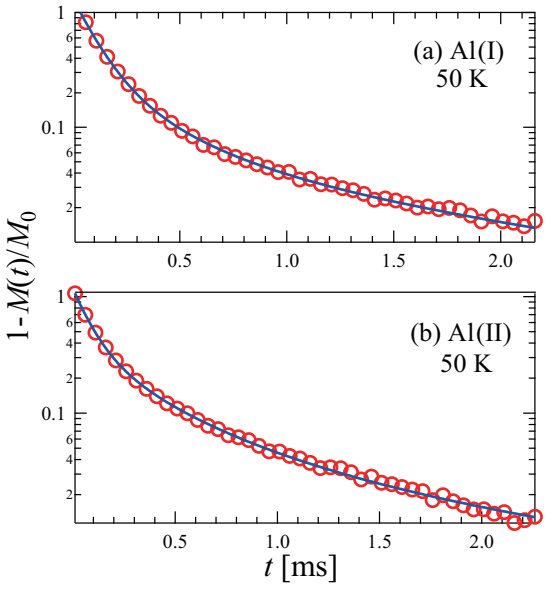


**Figure 7.** Nuclear longitudinal magnetization recovery $f(t) = 1 - (M(t)/M_0)$ of $^{27}$Al NMR in $EuAl_4$. Figs. (a) and (b) correspond to the Al(I) and Al(II) sites, respectively. The solid lines indicate the calculated results by using eq. (5).

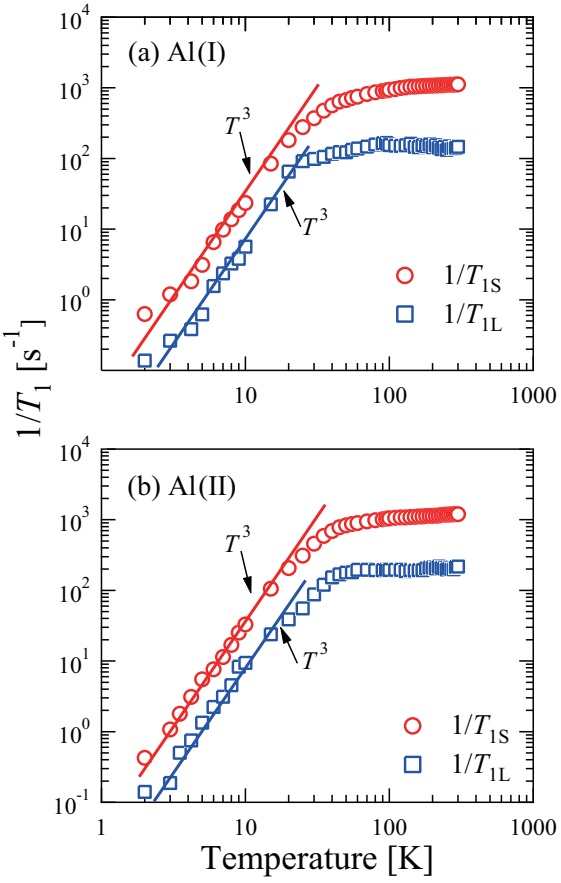


**Figure 8.** Temperature dependence of $1/T_1$ of $^{27}$Al NMR in $EuAl_4$. Figs. (a) and (b) correspond to the Al(I) and Al(II) sites, respectively.

The values of hyperfine fields $H_{\mathrm{hf\_iso}}$ and $H_{\mathrm{hf\_aniso}}$ are –3.231 and –0.162 kOe/$\mu_{\mathrm{B}}$ for Al(I) site and –1.823 and –0.264 kOe/$\mu_{\mathrm{B}}$ for Al(II) site, respectively. The ratio $H_{\mathrm{hf\_aniso}}/H_{\mathrm{hf\_iso}}$ is 4.99 % for Al(I) site and 14.48 % for Al(II) site, which is consistent with the ratio $K_{\mathrm{aniso}}(T)/K_{\mathrm{iso}}(T)$, respectively. It is found that the ratio $H_{\mathrm{hf\_aniso}}/H_{\mathrm{hf\_iso}}$ for Al(I) site is very small compared with that for Al(II) site and therefore the anisotropy of the Knight shift for Al(I) site is smaller than that for Al(II) site.

Spin-lattice relaxation time $T_1$ has been measured from 2 to 300 K. The nuclear longitudinal magnetization recovery $f(t) = 1-(M(t)/M_0)$ can be generally expressed by a single exponential type. However, as the structure is tetragonal symmetry, nuclear magnetic relaxation is affected by nuclear quadrupole interaction because $^{27}$Al nuclei has a nuclear spin of 5/2. Therefore, it can be expected that the nuclear magnetization recovery in the case of the transition $+1/2 \leftrightarrow$ -1/2 is analyzed by means of the following equation [12]:

$$f(t,T_1) = y\left\{\frac{1}{35}\exp\left(-\frac{t}{T_1}\right) + \frac{8}{45}\exp\left(-\frac{6t}{T_1}\right) + \frac{50}{63}\exp\left(-\frac{15t}{T_1}\right)\right\}, \tag{5}$$

where $y$ is an arbitrary constant. However, the recovery equation is slightly modified because $T_1$ is distributed. The recovery curve can be well explained by $g(t,T_1) = cf(t,T_{1\mathrm{S}})+(1-c)f(t,T_{1\mathrm{L}})$, consisting of two components of short $T_{1\mathrm{S}}$ and long $T_{1\mathrm{L}}$ as shown in Fig. 7. The values of $c$ are

about 0.9 for Al(I) site and about 0.8 for Al(II) site. The reason why $T_1$ is distributed in this material is not clear.

The values of spin-lattice relaxation rate $1/T_1$ for both Al(I) and Al(II) sites are almost constant in the vicinity of 300 K, since the random fluctuation of $f$-electron spins is fast in the paramagnetic states, while they are gradually decreased because of the slowdown of the fluctuation of the $f$-electron spins with decreasing temperature. Below 20 K, the $1/T_1$'s for both Al(I) and Al(II) sites are almost proportional to $T^3$. As the NMR measurements have been carried out in the external magnetic field of about 6.5 T, the antiferromagnetic state of $EuAl_4$ below $T_N = 16$ K is changed into the field induced ferromagnetic state as mentioned above. Therefore, the decay of $T^3$ in $1/T_1$ would be attributed to the excitation of the $f$ electron spins in the FRM ordered state. The change due to the CDW around 140 K in the $^{27}$Al NMR measurements cannot be detected because of the masking by the large magnetic moments of the $f$ electron spins.

In summary, in order to microscopically investigate the magnetic and electronic properties in $EuAl_4$, the $^{27}$Al NMR measurements have been carried out at temperatures between 2 and 300 K, applying an external magnetic field of approximately 6.5 T. In the paramagnetic phase, the $^{27}$Al NMR spectra for Al(I) and Al(II) sites are obtained. From the $^{27}$Al NMR spectra, the isotropic parts $K_{iso}$ and anisotropic part $K_{aniso}$ of the Knight shift, and nuclear quadrupole frequnces $\nu_Q$ are obtained for both sites. $K_{iso}$ and $K_{aniso}$ shift to negative side with decreasing temperature due to the RKKY interaction. These temperature dependences follow the Curie-Weiss law with $\theta_P = +14$ K, which is consistent with that of the magnetic susceptibility. From the $K - \chi$ plots, the values of the hyperfine fields $H_{hf\_iso}$ and $H_{hf\_aniso}$ are –3.231 and –0.162 kOe/$\mu_B$ for Al(I) site, and –1.823 and –0.264 kOe/$\mu_B$ for Al(II) site, respectively. The values of $\nu_Q$ of $^{27}$Al nucleus for Al(I) and Al(II) sites are approximately 0.865 and 0.409 MHz, respectively. The values of the nuclear relaxation rate $1/T_1$ of $^{27}$Al NMR for both sites is almost constant in the paramagnetic phase, while they are abruptly decreased in the ordered FRM state.

## References

[1] Bobev S, Bauer E D, Thompson J D, and Sarrao J L 2004 *J. Magn. Magn. Mater.* **277** 236.
[2] Nakamura A, Hiranaka Y, Hedo M, Nakama T, Miura Y, Tsutsumi H, Mori A, Ishida K, Mitamura K, Hirose Y, Sugiyama K, Honda F, Settai R, Takeuchi T, Hagiwara M, Matsuda T D, Yamamoto E, Haga Y, Matsubayashi K, Uwatoko Y, Harima H, and Ōnuki Y 2013 *J. Phys. Soc. Jpn.* **82** 104703.
[3] Wernick J H, Williams H J, and Gossard A C 1967 *J. Phys. Chem. Solids* **28** 271.
[4] Nakamura A, Hiranaka Y, Hedo M, Nakama T, Miura Y, Tsutsumi H, Mori A, Ishida K, Mitamura K, Hirose Y, Sugiyama K, Honda F, Takeuchi T, Matsuda T D, Yamamoto E, Haga Y, and Ōnuki Y 2014 *J. Phys. Soc. Jpn. Conf. Proc.* **3** 011012.
[5] Yogi M, Nakamura S, Higa N, Niki H, Hirose Y, Ōnuki Y, and Harima H 2013 *J. Phys. Soc. Jpn.* **82** 103701.
[6] Niki H, Nakamura S, Higa N, Yogi M, Hirose Y, Ōnuki Y, and Harima H 2014 *J. Phys. Soc. Jpn. Conf. Proc.* **3** 011015.
[7] Magishi K, Sugawara H, Takahashi M, Saito T, Koyama K, Saito T, Tatsuoka S, Tanaka K, and Sato H 2012 *J. Phys. Soc. Jpn.* **81** 124706.
[8] Yogi M, Niki H, Sugawara H, Takeda N, and Sato H 2011 *J. Phys. Soc. Jpn.* **80** SA027.
[9] Abragam A 1961 *The Principles of Nuclear Magnetism* (Oxford, U. K.: Oxford University Press).
[10] Aarts J, de Boer F R, Maclaughlin D E 1983 *Physica* B + C **121** 162.
[11] Ueda K, Kitaoka Y, Yamada H, Kohori Y, Kohara T, and Asayama K 1987 *J. Phys. Soc. Jpn.* **56** 867.
[12] Narath A 1967 *Phys. Rev.* **162** 320.